Revisiting the slow dynamics of a silica melt using Monte Carlo simulations

Ludovic Berthier*
Joint Theory Institute, Argonne National Laboratory and University of Chicago, 5640 South Ellis Avenue, Chicago, Illinois 60637, USA
(Received 18 May 2007; published 16 July 2007)

We implement a standard Monte Carlo algorithm to study the slow, equilibrium dynamics of a silica melt in a wide temperature regime, from 6100 K down to 2750 K. We find that the average dynamical behavior of the system is in quantitative agreement with results obtained from molecular dynamics simulations, at least in the long-time regime corresponding to the α-relaxation. By contrast, the strong thermal vibrations related to the boson peak present at short times in molecular dynamics are efficiently suppressed by the Monte Carlo algorithm. This allows us to reconsider silica dynamics in the context of mode-coupling theory, because several shortcomings of the theory were previously attributed to thermal vibrations. A mode-coupling theory analysis of our data is qualitatively correct, but quantitative tests of the theory fail, raising doubts about the very existence of an avoided singularity in this system. We discuss the emergence of dynamic heterogeneity and report detailed measurements of a decoupling between translational diffusion and structural relaxation, and of a growing four-point dynamic susceptibility. Dynamic heterogeneity appears to be less pronounced than in more fragile glass-forming models, but not of a qualitatively different nature.

DOI: 10.1103/PhysRevE.76.011507 PACS number(s): 64.70.Pf, 02.70.Ns, 05.20.Jj

I. INTRODUCTION

Numerical simulations play a major role among studies of the glass transition since, unlike in experimental works, the individual motion of a large number of particles can be followed at all times [1]. Computer simulations usually study Newtonian dynamics (ND) by solving a discretized version of Newton's equations for a given interaction between particles [2]. Although this is the most appropriate dynamics to study molecular liquids, it can be interesting to consider alternative dynamics that are not deterministic, or which do not conserve the energy. In colloidal glasses and physical gels, for instance, the particles undergo Brownian motion arising from collisions with molecules in the solvent, and a stochastic dynamics is more appropriate [2]. Theoretical considerations might also suggest the study of different sorts of dynamics for a given interaction between particles, for instance, to assess the role of conservation laws [3–5] and structural information [6,7]. Of course, if a given dynamics satisfies detailed balance with respect to the Boltzmann distribution, all structural quantities remain unchanged, but the resulting dynamical behavior might be very different. In this paper, we study the relaxation dynamics of a commonly used theoretical model for silica using Monte Carlo simulations and compare the results with previous ND studies for both the averaged dynamical behavior and the spatially heterogeneous dynamics of this system.

Several papers have studied in detail the influence of the chosen microscopic dynamics on the dynamical behavior in a simple glass former, namely a binary mixture of Lennard-Jones particles [1,8]. Gleim, Kob, and Binder [9] studied stochastic dynamics where a friction term and a random noise are added to Newton's equations, the amplitude of both terms being related by a fluctuation-dissipation theorem. Szamel and Flenner [10] used Brownian dynamics, in which there are no momenta, and positions evolve with Langevin dynamics. Berthier and Kob [11] employed Monte Carlo dynamics, where the potential energy between two configurations is used to accept or reject a trial move. The equivalence between these three stochastic dynamics and the originally studied ND was established at the level of the averaged dynamical behavior, except at very short times where differences are indeed expected. However, important differences were found when dynamic fluctuations were considered, even in the long-time regime comprising the α relaxation [3,4,11].

Silica, the material studied in the present work, is different from the previously considered Lennard-Jones case in many aspects which all motivate our Monte Carlo study of the van Beest, Kramer, and van Santen (BKS) model for silica [12]. First, the BKS model was devised to represent a real material, making our conclusions more directly applicable to experiments. Second, the temperature evolution of relaxation times is well described by a simple Arrhenius law at low temperatures, typical of strong glass formers, which are commonly believed to belong to a somewhat different class of materials, so that qualitative differences might be expected with more fragile, super-Arrhenius relaxing materials. Third, the onset of slow dynamics in fragile materials is often said to be accurately described by the application of mode-coupling theory, at least over an intermediate window of 2 to 3 decades of relaxation times [7]. Mode-coupling theory (MCT) formulates in particular a series of quantitative predictions regarding the time, spatial, and temperature dependences of dynamic correlators. In the case of silica melts, previous analysis reported evidence in favor of a narrower temperature regime where MCT can be applied, but the test of several theoretical predictions was either seriously affected, or even made impossible by the presence of strong short-time thermal vibrations related to the boson peak in this material [13]. These vibrations affect the time dependence of the correlators much more strongly in silica than in

*Permanent address: Laboratoire des Colloïdes, Verres et Nanomatériaux, UMR 5587, Université Montpellier II and CNRS, 34095 Montpellier, France.

Lennard-Jones systems, which constitutes a fourth difference between the two systems. Using Monte Carlo simulations we shall therefore be able to revisit the MCT analysis performed in Ref. [13]. Fifth, while detailed analysis of dynamic heterogeneity is available for fragile materials, a comparatively smaller amount of data is available for strong materials [3,4,14,15], and we shall therefore investigate issues that have not been addressed in previous work.

The paper is organized as follows. In Sec. II we give details about the simulation technique and compare its efficiency to previously studied dynamics. In Sec. III we present our numerical results about the averaged dynamics of silica in Monte Carlo simulations, while Sec. IV deals with aspects related to dynamic heterogeneity. Finally, Sec. V concludes the paper.

II. SIMULATING SILICA USING MONTE CARLO DYNAMICS

Our aim is to study a non-Newtonian dynamics of the glass-former silica, SiO_2. Therefore, we must first choose a reliable model to describe the interactions in this two-component system made of Si and O atoms, and then design a specific stochastic dynamics which we require to be efficient and to yield the same static properties as Newtonian dynamics.

Various simulations have shown that a reliable pair potential to study silica in computer simulations is the one proposed by BKS [12–18]. The functional form of the BKS potential is

$$\phi_{\alpha\beta}^{\mathrm{BKS}}(r) = \frac{q_\alpha q_\beta e^2}{r} + A_{\alpha\beta}\exp(-B_{\alpha\beta}r) - \frac{C_{\alpha\beta}}{r^6}, \qquad (1)$$

where $\alpha,\beta \in [\mathrm{Si},\mathrm{O}]$ and r is the distance between the atoms of type α and β. The values of the constants q_α, q_β, $A_{\alpha\beta}$, $B_{\alpha\beta}$, and $C_{\alpha\beta}$ can be found in Ref. [12]. For the sake of computational efficiency the short-range part of the potential was truncated and shifted at 5.5 Å. This truncation also has the benefit of improving the agreement between simulation and experiment with regard to the density of the amorphous glass at low temperatures. The system investigated has $N_{\mathrm{Si}}=336$ and $N_{\mathrm{O}}=672$ atoms in a cubic box with fixed size $L=24.23$ Å, so that the density is $\rho=2.37$ g/cm^3, close to the experimentally measured density at atmospheric pressure of 2.2 g/cm^3 [19].

Once the pair interaction is chosen, we must decide what stochastic dynamics to implement. Previous studies in a Lennard-Jones system concluded that among Monte Carlo (MC), stochastic dynamics (SD) and Brownian dynamics (BD), MC was by far the most efficient algorithm because relatively larger incremental steps can be used while maintaining detailed balance, which is impossible for SD and BD where very small discretized time steps are needed to maintain the fluctuation-dissipation relation between noise and friction terms [11]. Given the generality of this argument, it should carry over to silica, and we decided to implement MC dynamics to the BKS model. An additional justification for our choice stems from results by Horbach and Kob who performed preliminary investigations of the SD of BKS silica [20]. Using a friction term similar in magnitude to the one used in Lennard-Jones simulations was however not enough to efficiently suppress short-time elastic vibrations. Using an even larger friction term would probably damp these vibrations, but would also make the simulation impractically slow.

A standard Monte Carlo dynamics [2] for the pair potential in Eq. (1) should proceed as follows. In an elementary MC move, a particle, i, located at the position $\mathbf{r}_i$ is chosen at random. The energy cost, ΔE_i, to move particle i from position $\mathbf{r}_i$ to a new, trial position $\mathbf{r}_i+\delta\mathbf{r}$ is evaluated, $\delta\mathbf{r}$ being a random vector comprised in a cube of linear length $\delta_{\max}$ centered around the origin. The Metropolis acceptance rate, $p=\min(1,e^{-\beta\Delta E_i/k_B})$, where $\beta=1/T$ is the inverse temperature, is then used to decide whether the move is accepted or rejected. In the following, one Monte Carlo time step represents $N=N_{\mathrm{Si}}+N_{\mathrm{O}}$ attempts to make such an elementary move, and time scales are reported in this unit. Temperature will be expressed in Kelvin. Monte Carlo simulations can of course be made even more efficient by implementing, for instance, swaps between particles, or using parallel tempering. The dynamical behavior, however, is then strongly affected by such nonphysical moves and only equilibrium thermodynamics can be studied. Since we want to conserve a physically realistic dynamics, we cannot use such improved schemes.

An additional difficulty with Eq. (1) as compared to Lennard-Jones systems is the Coulombic interaction in the first term. Such a long-range interaction means that the evaluation of the energy difference ΔE_i needed to move particle i in an elementary MC step requires a sum over every particle $j\neq i$, and over their repeated images due to periodic boundary conditions. Of course, the sum can be efficiently evaluated using Ewald summations techniques, as is commonly employed in ND simulations [2]. We note, however, that Ewald techniques are better suited for ND than for MC since in ND the positions and velocities of all particles are simultaneously updated so that the Ewald summation is performed once to update all particles. In MC simulations, each single move requires its own Ewald summation, and this remains computationally very costly.

For the BKS potential in Eq. (1) it was recently shown that a simple truncation can be performed which makes the range of the Coulombic interaction term finite [21]. Detailed ND simulations have shown that in the range of temperatures presently accessible to computer experiments, no difference can be detected between the finite range and the infinite range versions of the BKS potential for a wide variety of static and dynamic properties. Therefore we build on this work and make the replacement [21]

$$\frac{1}{r} \to \left(\frac{1}{r}-\frac{1}{r_c}\right) + \frac{1}{r_c^2}(r-r_c) \quad \text{for } r \leqslant r_c, \qquad (2)$$

while $1/r\to 0$ for $r>r_c$. This amounts to smoothly truncating the potential at a finite range, r_c, maintaining both energy and forces continuous at the cutoff $r=r_c$. The physical motivation for this form of the truncation was given by Wolf [22], and discussed in several more recent papers [21,23]. Following Ref. [21], we fix $r_c=10.14$ Å. Once the potential is trun-

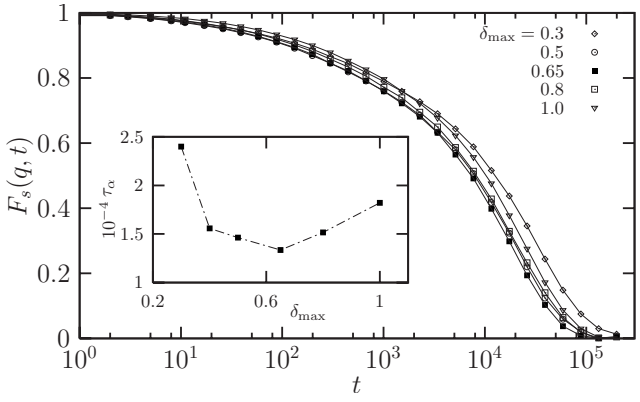

FIG. 1. Self-intermediate scattering function for silicon, Eq. (3), at $T=4000$ K and $|\mathbf{q}|=1.7$ Å^{-1} for various values of δ_{max}. Inset: The evolution of the relaxation time with δ_{max} unambiguously defines an optimal value $\delta_{max}\approx 0.65$ Å for efficient Monte Carlo simulations.

cated, MC simulations become much more efficient, and much simpler to implement. Furthermore, this will allow us to perform detailed comparisons of the dynamics of the BKS model of silica where the Wolf truncation is used for both ND and MC in the very same manner, so that any difference between the two sets of data can be safely assigned to the change of microscopic dynamics alone, while reference to earlier work done using Ewald summations is still quantitatively meaningful.

The one degree of freedom that remains to be fixed is δ_{max}, which determines the average length scale of elementary moves. On the one hand, chosen too small, energy costs are very small and most of the moves are accepted, but the dynamics is very slow because it takes a long time for particles to diffuse over the long distances needed to relax the system. On the other hand, too large displacements will on average be very costly in energy and acceptance rates can become prohibitively small. We seek a compromise between these two extremes by monitoring the dynamics at a moderately low temperature, $T=4000$ K, for several values of δ_{max}. As a most sensitive indicator of the relaxational behavior, we measure the contribution from the specie α (α=Si, O) to the self-intermediate scattering function defined by

$$F_s(q,t) = \left\langle \frac{1}{N_\alpha} \sum_{j=1}^{N_\alpha} e^{i\mathbf{q}\cdot[\mathbf{r}_j(t)-\mathbf{r}_j(0)]} \right\rangle. \tag{3}$$

We make use of rotational invariance to spherically average over wave vectors of comparable magnitude, and present results for $|\mathbf{q}|=1.7$ Å^{-1}, which is the location of the prepeak observed in the static structure factor $S(q)$ of the liquid. This corresponds to the typical (inverse) size of the SiO_4 tetrahedra. In Fig. 1 we present our results for δ_{max} values between 0.3 and 1.0 Å. As expected we find that relaxation is slow both at small and large values of δ_{max}, and most efficient for intermediate values. Interestingly we also note that the overall shape of the self-intermediate scattering function does not sensitively depend on δ_{max} over this wide range. We can

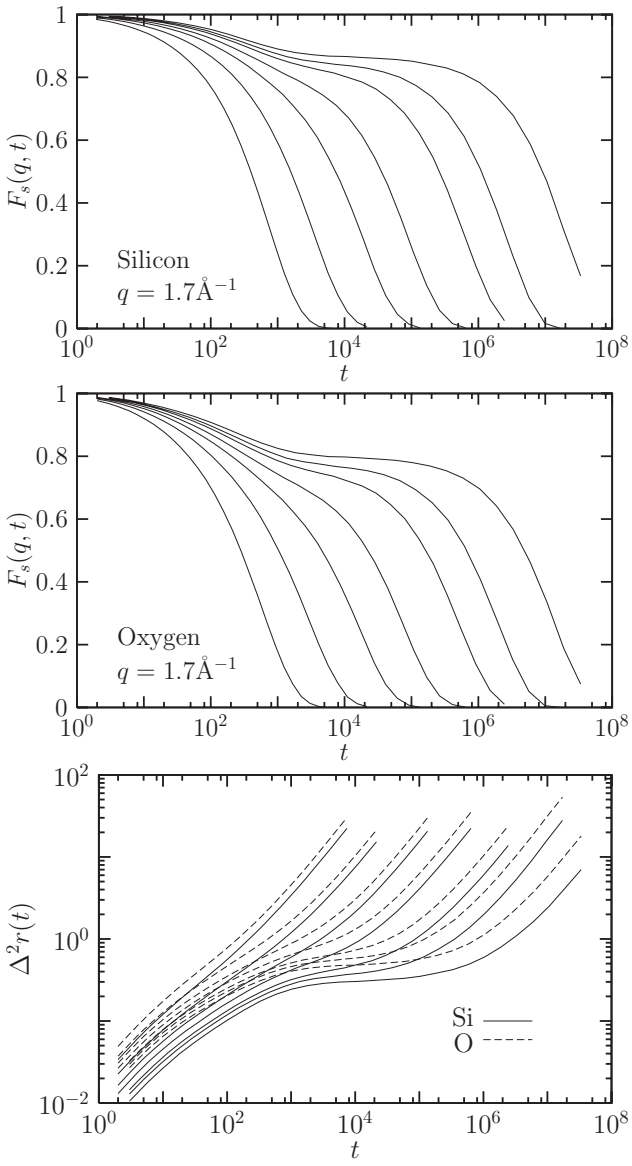

FIG. 2. Top: Self-intermediate scattering function, Eq. (2), for $|\mathbf{q}|=1.7$ Å^{-1} and temperatures $T=6100$, 4700, 4000, 3580, 3200, 3000, and 2750 K (from left to right). Bottom: Mean-squared displacement, Eq. (5), for the same temperatures in the same order.

therefore safely fix the value of δ_{max} based on an efficiency criterium alone.

We define a typical relaxation time, τ_α, as

$$F_s(q,\tau_\alpha) = \frac{1}{e}, \tag{4}$$

and show its δ_{max} dependence in the inset of Fig. 1. A clear minimum is observed at the optimal value of $\delta_{max}\approx 0.65$ Å, which we therefore use throughout the rest of this paper. This distance corresponds to a squared displacement of 0.4225 Å^2, which is very close to the plateau observed at intermediate times in the mean-squared displacements (see Fig. 2 below). This plateau can be taken as a rough measurement of the "cage" size for the particles, so that MC simu-

lations are most efficient when the cage is most quickly explored. This argument and the data in Fig. 2 suggest that the location of the minimum should only be a weak function of temperature, but we have not verified this point in detail. Therefore we keep the value of $\delta_{\max}$ constant at all temperatures. An alternative would be to optimize it at each T and then carefully rescale time scales between runs at different temperatures.

What about the relative efficiency between MC and ND? If we compare the relaxation measured at $T=4000$ K, we find $\tau_\alpha \sim 13\,400$ Monte Carlo steps, while $\tau_\alpha \sim 4.7$ ps for ND. When using a discretized time step of 1.6 fs, this means that, when counting in number of integration time steps, MC dynamics is ≈ 5 times slower than ND. This result contrasts with the results obtained in a Lennard-Jones mixture where MC dynamics was about 2 times faster than ND [11]. We attribute this relative loss of efficiency to the existence of strong bonds between Si and O atoms in silica, which have no counterparts in Lennard-Jones systems. It is obvious that strong bonds are very hard to relax when using sequential Monte Carlo moves, as recently discussed in Ref. [24].

We have performed simulations at temperatures between $T=6100$ K and $T=2750$ K, the latter being smaller than the fitted mode-coupling temperature, $T_c=3330$ K [13]. For each temperature we have simulated three independent samples to improve the statistics. Initial configurations were taken as the final configurations obtained from previous work performed with ND [21], so that production runs could be started immediately. For each sample, production runs lasted at least $15\tau_\alpha$ (at $T=2750$ K), much longer for higher temperatures, so that statistical errors in our measurements are fairly small. We have performed a few runs for a larger number of particles, namely $N=8016$ particles, to investigate finite size effects which are known to be relevant in silica [25–27], and the results will be discussed in Sec. III.

III. ANALYSIS OF AVERAGED TWO-TIME CORRELATORS

In this section we report our results about the time behavior of averaged two-time correlators, we compare the Monte Carlo results to Newtonian dynamics, and we perform a quantitative mode-coupling analysis of the data.

A. Intermediate scattering function and mean-squared displacements

The self-intermediate scattering function, Eq. (3), is shown in Fig. 2 for temperatures decreasing from $T=6100$ K down to $T=2750$ K for Si and O atoms at $|\mathbf{q}|=1.7$ Å^{-1}. These curves present well-known features. Dynamics at high temperature is fast and has an exponential nature. When temperature is decreased below $T\approx 4500$ K, a two-step decay, the slower being strongly nonexponential, becomes apparent. Upon decreasing the temperature further, the slow process dramatically slows down by about 4 decades, while clearly conserving an almost temperature-independent, nonexponential shape, as already reported for ND [13].

We also find that the first process, the decay towards a plateau, slows down considerably when decreasing temperature, although less dramatically than the slower process. The fastest process, called critical decay in the language of mode-coupling theory [7], is not observed when using ND, because it is obscured by strong thermal vibrations occurring at high frequencies (in the THz range). Clearly, no such vibrations are detected in the present results which demonstrates our first result: MC simulations very efficiently suppress the high-frequency oscillations observed with ND.

Although the plateau seen in $F_s(q,t)$ is commonly interpreted as vibrations of a particle within a cage, the data in Fig. 2 discard this view. From direct visualization of the particles' individual dynamics it is obvious that vibrations take place in just a few MC time steps, while the decay towards the plateau can be as long as 10^4 time units at the lowest temperatures studied here. This decay is therefore necessarily more complex, most probably cooperative in nature. This interpretation is supported by recent theoretical studies where a plateau is observed in two-time correlators of lattice models where local vibrations are indeed completely absent [28]. A detailed atomistic description of this process has not yet been reported, but would indeed be very interesting.

Next, we study the mean-squared displacement defined as

$$\Delta^2 r(t) = \frac{1}{N_\alpha} \sum_{i=1}^{N_\alpha} \langle |\mathbf{r}_i(t) - \mathbf{r}_i(0)|^2 \rangle, \tag{5}$$

and we present its temperature evolution in Fig. 2, for both Si and O atoms. The evolution of $\Delta^2 r(t)$ mirrors that of the self-intermediate scattering function, and the development of a two-step relaxation process is clear from these figures. Because we are studying stochastic dynamics, displacements are diffusive at both short and long time scales. This constitutes an obvious, expected difference between ND and MC simulations: data clearly cannot match at very small times. The goal of the present study is therefore to determine whether the dynamics quantitatively match at times where the relaxation is not obviously ruled by short-time ballistic and/or diffusive displacements.

The plateau observed in $F_s(q,t)$ now translates into a strongly subdiffusive regime in the mean-squared displacements separating the two diffusive regimes. At the lowest temperature studied, when t changes by three decades from 2×10^2 to 2×10^5, the mean-squared displacement of Si changes by a mere factor 2.8 from 0.14 to 0.39. Particles are therefore nearly arrested for several decades of times, before eventually entering the diffusing regime where the relaxation of the structure of the liquid takes place.

B. Comparison to Newtonian dynamics

The preceding subsection has shown that the Monte Carlo dynamics of silica is qualitatively similar to the one reported for ND, apart from relatively short times where the effect of thermal vibrations is efficiently suppressed and the dynamics is diffusive instead of ballistic. We now compare our results more quantitatively with the dynamical behavior observed using ND.

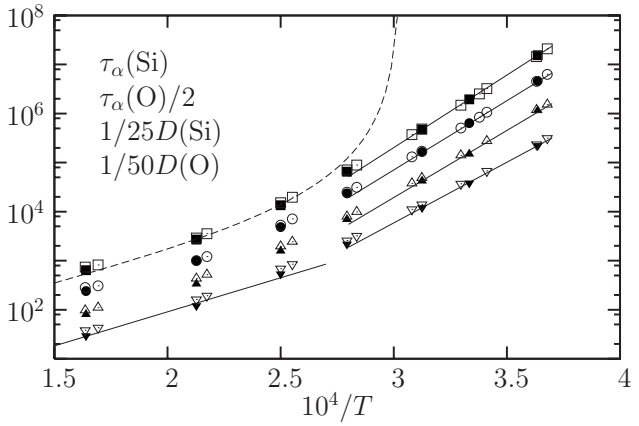

FIG. 3. Temperature evolution of the α-relaxation time $\tau_\alpha(T)$ for silicon (squares) and oxygen (circles), and inverse self-diffusion constant for silicon (up triangles) and oxygen (down triangles), vertically shifted for clarity. Open symbols are for ND (times rescaled by t_0=0.31 fs) closed symbols for MC. Full lines are Arrhenius fits below $T\approx3700$ K with activation 5.86, 5.60, 5.43, and 4.91 eV (from top to bottom). An Arrhenius fit for high temperatures is also presented for D(O) with activation energy 2.76 eV. The dashed line is a power law fit, $\tau_\alpha\sim(T-T_c)^{-\gamma}$, with T_c=3330 K and γ=2.35.

To this end, we compare first the temperature evolution of the relaxation times, $\tau_\alpha(T)$, defined in Eq. (4), in Fig. 3. Here, we use a standard representation where an Arrhenius slowing down over a constant energy barrier E, with an attempt frequency $1/\tau_0$,

$$\tau_\alpha = \tau_0 \exp\left(\frac{E}{k_B T}\right), \tag{6}$$

appears as a straight line. To compare both sets of data we rescale the ND data by a common factor, t_0=0.31 fs, which takes into account the discretization time step and the efficiency difference discussed in the preceding section; t_0 will be kept constant throughout this paper. We find that the temperature evolution of the α-relaxation time measured in MC simulations is in complete quantitative agreement with the one obtained from ND, over the complete temperature range. This proves that Monte Carlo techniques can be applied not only to study static properties of silica, but also its long-time dynamic properties.

In Fig. 3 we also show the temperature evolution of the self-diffusion constant, defined from the long-time limit of the mean-squared displacement as

$$D = \lim_{t\to\infty} \frac{\Delta^2 r(t)}{6t}. \tag{7}$$

The behavior of the (inverse) diffusion constant is qualitatively very close to the one of the α-relaxation time, and we again find that ND and MC dynamics yield results in full quantitative agreement.

As expected for silica, we find that at low temperatures below $T\approx3700$ K, relaxation time scales and diffusion constant change in an Arrhenius fashion described by Eq. (6). We find, however, that the observed activation energies display small variations between different observables, from 5.86 eV for τ_α(Si) to 4.91 eV for $1/D(0)$. These values compare well with previous analysis [13], and with experimental findings [29].

From Fig. 3, it is clear that Arrhenius behavior is obeyed below $T\approx3700$ K only, while the data bend up in this representation for higher temperatures. This behavior was interpreted in terms of a fragile to strong behavior of the relaxation time scales in several papers [13,30,31], despite the fact that fragility is usually defined experimentally by considering data on a much wider temperature window close to the experimental glass transition. To rationalize these findings, Horbach and Kob analyzed the data using mode-coupling theory predictions [13]. In particular they suggest to fit the temperature dependence of τ_α as

$$\tau_\alpha \sim (T - T_c)^{-\gamma}, \tag{8}$$

with $T_c\approx3330$ K and $\gamma\approx2.35$. This power law fit is also presented in Fig. 3 as a dashed line. Its domain of validity is of about 1 decade, which is significantly less than for more fragile materials with super-Arrhenius behavior of relaxation time scales [8].

It is interesting to note that a simpler interpretation of this phenomenon could be that this behavior is nothing but a smooth crossover from a nonglassy, homogeneous, high-temperature behavior to a glassy, heterogeneous, low temperature behavior, as found in simple models of strong glass-forming liquids [32]. In Fig. 3, we implement this simpler scenario by fitting high temperature data with an Arrhenius law, as is sometimes done in the analysis of experimental data [33]. Such a fit works nicely for high temperatures, from T=6100 to 4700 K, but breaks down below $T\approx4000$ K. A physical interpretation for this high-temperature Arrhenius behavior was offered in Ref. [34]. This shows that analyzing silica dynamics in terms of a simple crossover occurring around 4000 K between two simple Arrhenius law is indeed a fair description of the data which does not require invoking a more complex fragile to strong crossover being rationalized by the existence of an avoided mode-coupling singularity.

The difference found above for the activation energies describing τ_α and $1/D$ for both species implies that these quantities, although both are devised to capture the temperature evolution of single particle displacements, have slightly different temperature evolutions and are not proportional to one another. This well-known feature implies the existence of a "decoupling" between translational diffusion and structural relaxation in silica, as documented in previous papers [13]. In Fig. 4 we report the temperature evolution of the product $D(T)\tau_\alpha(q,T)$ which is a pure constant for a simply diffusive particle where $\tau_\alpha(q,T)=1/(q^2D)$. We normalize this quantity by its value at T_o=4700 K, so that any deviations from 1 indicates a nonzero decoupling [35,36]. As expected we find that the product is not a constant, but grows when temperature decreases. Remarkably, although this quantity is a much more sensitive probe of the dynamics of the liquid, its temperature evolution remains quantitatively similar for both ND and MC dynamics. This shows that equivalence of the dynamics between the two algorithms

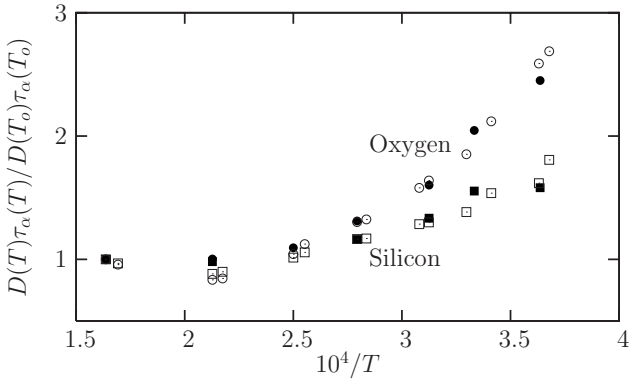

FIG. 4. Decoupling data for oxygen and silicon. We plot the product $D\tau_\alpha$ taken from the data shown in Fig. 3 and normalize the product by its value at T_o=4700 K such that deviations from 1 indicates nonzero decoupling. Open symbols are for ND, closed symbols for MC. Decoupling is similar for both types of dynamics.

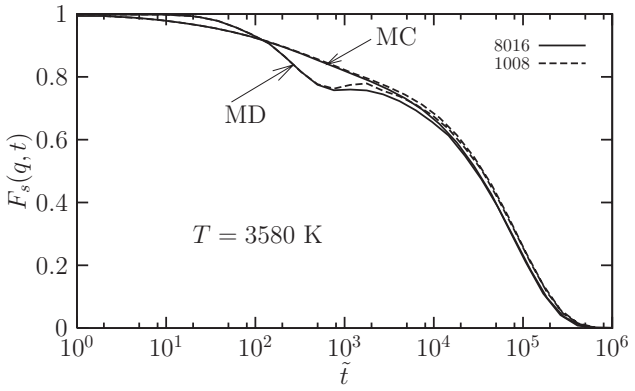

FIG. 5. Self-intermediate scattering function for fixed T and q =1.7 Å^{-1}, obtained in MC and MD simulations for two system sizes. The time axis in MD data is rescaled by t_0=0.31 fs to obtain maximum overlap with MC results, and the same factor is used for the two sizes. Larger systems relax faster and the amplitude of this finite size effect is the same for both dynamics.

holds at the level of the complete distribution of particle displacements, even for those tails that are believed to dictate the observed decoupling.

In Sec. IV, we shall explore in more detail the heterogeneous character of the dynamics of silica, closely related to the decoupling discussed here. It is however interesting to try and infer the amount of decoupling predicted for silica at temperatures close to the experimental glass transition, $T_g \approx 1450$ K. The glass transition temperature of BKS silica deduced from extrapolation of viscosity measurements is close to the experimental one, $T_g^{\mathrm{BKS}} \approx 1350$ K [13]. Extrapolating the data in Fig. 4 down to 1400 K predicts a decoupling of about 40 for Si dynamics, about 7 for O dynamics. The difference between Si and O dynamics was recently explained in Ref. [34], where it was noted that oxygen diffusion is in fact possible with no rearrangement of the tetrahedral structure of silica involved. Moreover, it is interesting to note that the amount of decoupling found here is smaller than experimental findings in fragile materials close to their glass transition [37], but is nonetheless clearly different from zero. This suggests that even strong materials display dynamically heterogeneous dynamics, but its effect seems less pronounced than in more fragile materials.

Theoretically, an identical temperature evolution of the α-relaxation time scale for MC and ND is an important prediction of mode-coupling theory [7] because the theory uniquely predicts the dynamical behavior from static density fluctuations. Gleim *et al.* argue that their finding of a quantitative agreement between SD and ND in a Lennard-Jones mixture is a nice confirmation of this nontrivial mode-coupling prediction [9]. Szamel and Flenner [10] confirmed this claim using BD, and argued further that even deviations from mode-coupling predictions are identical, a statement that was extended to below the mode-coupling temperature by Berthier and Kob [11]. In the present work we extend these findings to the case of silica over a large range of temperatures, which goes far beyond the temperature regime where MCT can be applied. Therefore, we conclude that such an independence of the glassy dynamics of supercooled liquids to their microscopic dynamics, although predicted by MCT, certainly has a much wider domain of validity than the theory itself. Finally, we note that the deviations from MCT predictions observed in Fig. 3 cannot be attributed to coupling to currents which are expressed in terms of particle velocities. In our MC simulations we have no velocities, so that avoiding the mode-coupling singularity is not due to the hydrodynamic effects pointed out in Ref. [5] (see Ref. [38] for more recent theoretical viewpoints).

The last comparison to ND we want to discuss concerns the study of finite size effects. It was shown that the long-time dynamics of silica is fairly sensitive to system size, and there are detectable differences when the number of particles is changed from 1000 to 8000 [25,27]. Such a large effect is not observed in more fragile materials [8]. It was suggested that short-time thermal vibrations, stronger in silica than in simpler models, are responsible for this system size dependence [27,39]. Therefore, it could be expected that by efficiently suppressing these vibrations, finite size effects should be reduced. But this is not what happens. In Fig. 5, we show self-intermediate scattering functions measured at T =3580 K and $|\mathbf{q}|$=1.7 Å^{-1} in both ND and MC for two system sizes, N=1008 and N=8016 particles. Such data have been presented for ND before [27], and our results agree with these earlier data. The amplitude of the vibrations observed for $t/t_0=\tilde{t} \approx 10^3$ is smaller and the long-time dynamics is faster when N is larger. For MC we find that high-frequency vibrations and the corresponding finite size effects are indeed suppressed, but the finite size effect for long-time relaxation, somewhat surprisingly, survives in our MC simulations, and can therefore not be attributed to high-frequency thermal vibrations. Recent studies of the vibration spectrum and elastic properties at T=0 of amorphous media have suggested the existence of large-scale structures [40]: these objects are potential candidates to account for the size effect found at long times. It should then be explained how these spatial structures affect the long time dynamics, and why a finite size simulation box at the same time affects the absolute value of the α-relaxation time scale but leaves unchanged many of its detailed properties [26,41].

C. Mode-coupling analysis of dynamic correlators

We now turn to a more detailed analysis of the shape and wave vector dependences of two-time correlation functions, revisiting in particular the mode-coupling analysis performed by Horbach and Kob in Ref. [13]. They argue that MCT can generally be applied to describe their silica data, and attribute most of the deviations that they observe to short-time thermal vibrations supposedly obscuring the "true" MCT behavior. We are therefore in a position to verify if their hypothesis is correct.

When applied to supercooled liquids, MCT formulates a series of detailed quantitative predictions regarding the time, wave vector, and temperature dependences of two-time dynamical correlators close to the mode-coupling singularity. In particular, MCT predicts that correlation functions should indeed decay in the two-step manner reported in Fig. 2. Moreover, for intermediate times corresponding to the plateau observed in correlation functions, an approximate equation can be derived which describes the correlator close enough to the plateau [7]. The following behavior is then predicted,

$$F_s(q,t) \approx f_q + h_q F(t), \tag{9}$$

where $F(t)$ is the so-called β correlator which is independent of the wave vector, and whose shape depends on a few parameters: the reduced distance from the mode-coupling temperature, $\epsilon = |T - T_c|/T_c$, and a parameter describing the MCT critical exponents, λ. Once λ is known various exponents (a, b, γ) are known, which describe, in particular, the short-time behavior of $F(t)$ when $F_s(q,t)$ approaches the plateau, $F(t) \sim t^{-a}$, and its long-time behavior when leaving the plateau, $F(t) \sim t^{b}$. The exponent γ was introduced in Eq. (8) and describes the temperature evolution of the relaxation time τ_α.

Several properties follow from Eq. (9). If one works at fixed temperature and varies the wave vector, the following quantity,

$$R(t) \equiv \frac{\phi(t) - \phi(t')}{\phi(t'') - \phi(t')} \approx \frac{F(t) - F(t')}{F(t'') - F(t')}, \tag{10}$$

where $\phi(t)$ stands for a two-time correlation function, should become independent of q. In Eq. (10), t' and t'' are two arbitrary times taken in the plateau regime. This is called the "factorization property" in the language of MCT. We follow Ref. [13] and show in Fig. 6 the function $R(t)$ in Eq. (10) using self-intermediate scattering functions for different q and for different species (Si and O) at fixed temperatures, $T=3580$ K and $T=3000$ K, choosing times comparable to those reported in Ref. [13], namely $t''=82$ and $t'=760$ for $T=3580$ K, and $t''=1360$ and $t'=66700$ for $T=3000$ K. Although the factorization property seemed to hold quite well in the ND data, this is no more the case for our MC data, and $R(t)$ retains a clear q dependence between t' and t'': no collapse of $R(t)$ can be seen in the regime $t' < t < t''$ in Fig. 6. The reason is clear from Fig. 2: due to thermal vibrations, the intermediate plateau was very flat in ND, but it has much more structure in our MC data. It was therefore easier to collapse the ND data in this regime than the present MC data for which a better agreement might have been expected. In the case of the factorization property, the presence of thermal vibrations in fact favors a positive reading of the data, which become much less convincing when these vibrations are suppressed. Gleim and Kob had reached an opposite conclusion in the case of a Lennard-Jones system [42]. They found that suppressing vibrations made the mode-coupling analysis of the beta-relaxation more convincing, suggesting that MCT describes the Lennard-Jones system more accurately than silica.

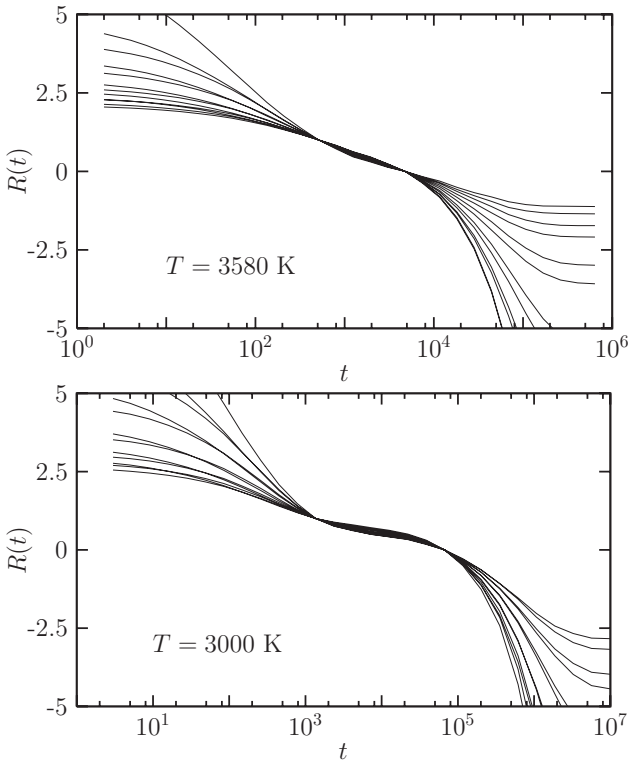

FIG. 6. Test of the factorization property, Eq. (10) using $F_s(q,t)$ from Si and O dynamics, and wave vectors between 0.8 and 4 Å^{-1}, for $T=3580$ K and 3000 K. The data do not show collapse for times $t' < t < t''$, and factorization does not work very well.

Next we perform a test of the theory which had not been possible with ND data. We investigate in detail if the behavior predicted by Eq. (9) is correct for both short and long times. This test is not possible using ND because the approach to the plateau is mainly ruled by thermal vibrations (see, for instance, the ND data presented in Fig. 5). In Fig. 7 we show that a "critical decay" does indeed show up when thermal vibrations are overdamped and no oscillations can be seen. To check in more detail if this behavior is indeed in quantitative agreement with the MCT predictions, we fit the $F_s(q,t)$ data at $T=3580$ K, i.e., slightly above $T_c=3330$ K, for several wave vectors q using the β correlator obtained from numerical integration of the mode-coupling equation. To get the fits shown in Fig. 7 we must fix the distance to the mode-coupling temperature ϵ and the value $\lambda=0.71$ both taken from Ref. [13], and yielding $a=0.32$, $b=0.62$, and $\gamma=2.35$. Additionally we must adjust the microscopic time scale. Moreover, for each wave vector we must fix h_q and f_q which, respectively, correspond to the amplitude of the β correlator and the height of the plateau in $F_s(q,t)$. Finally,

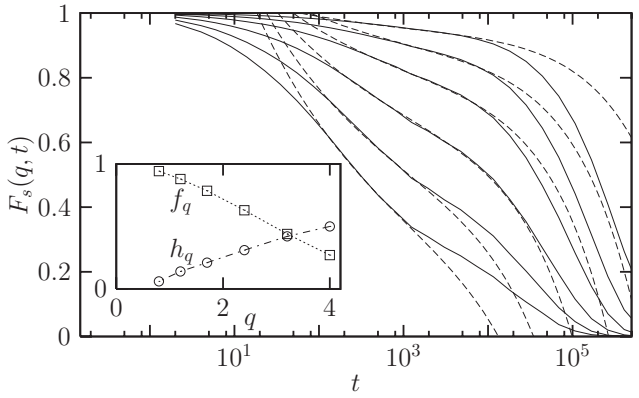

FIG. 7. Self-intermediate scattering function at fixed $T=3580$ K and various wave vectors, $q=0.8$, 1.2, 1.7, 2.4, 3.2, and 4 Å^{-1} (from right to left). Dashed lines show fits at intermediate times using Eq. (9). The inset shows the q dependence of the fitting parameters h_q and f_q. Note that the time domains over which the fits apply shift with q.

there are two additional "hidden" free parameters in each of these fits: the somewhat arbitrarily chosen boundaries of the time domain where the fitting function describes the data. We then get the fits shown with dashed lines in Fig. 7, which are of a quality comparable to the ones usually found in the MCT literature [7]. The parameters h_q and f_q are also shown in the inset of Fig. 7, and behave qualitatively as in similar studies. Inspection of Fig. 7 reveals that the use of such freedom to fit the data allows a qualitatively correct description of the data, although clearly the time domain over which each wave vector is fit systematically shifts when q changes, and we could not simultaneously fit the data at both small and large q by fixing the time interval of the fit. This failure is consistent with the above finding that the factorization property is not satisfied.

Therefore we conclude that MCT provides a qualitatively correct description of our data in the plateau regime, with no satisfying quantitative agreement, even in the absence of short-time thermal vibrations. One must therefore argue that the data are taken too far from the transition for MCT to quantitatively apply to silica. However, since it is not possible to get data closer to the transition (recall that the transition does not exist), the domain of validity of the theory then would become vanishingly small.

We now turn to longer time scales and show in Fig. 8 a test of the time-temperature superposition prediction of the theory which states that correlators at fixed q but different temperatures should scale as [7]

$$F_s(q,t) \approx \mathcal{F}_q\left(\frac{t}{\tau_\alpha(q)}\right), \tag{11}$$

where $\mathcal{F}_q(x) \approx f_q \exp(-x^{\beta(q)})$ and for times in the α regime. When high temperatures outside the glassy regime are discarded Eq. (11) works correctly when the scaling variable t/τ_α is not too small, but fails more strongly in the late β regime. Scaling in the β regime is often one of the most successful predictions of MCT, see, e.g., Ref. [8]. In the

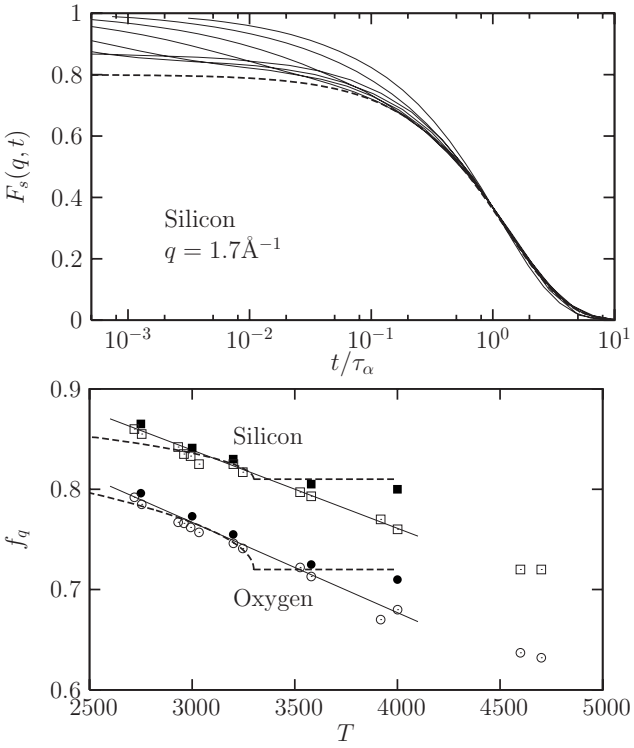

FIG. 8. Top: Test of time-temperature superposition, Eq. (11). The dashed line is a stretched exponential function with $\beta=0.87$. Superposition holds at large rescaled times, but fails in the β regime because the plateau height increases when T decreases. Bottom: Extracted plateau height as a function of temperature fitted with a linear dependence (full line) and with a square root singularity, Eq. (12) (dashed line). Open symbols are for ND, closed symbols for MC. No singular behavior of f_q is visible in either set of data.

present case, it could be argued to fail because we are collapsing data at temperatures which are both above and below T_c. Indeed, below T_c scaling in the β regime is not expected anymore because the height of the plateau, f_q in Eq. (9), now becomes a temperature dependent quantity, with the following predicted singular behavior [7]:

$$f_q(T) = f_q(T_c) + \alpha\sqrt{T_c - T}, \quad T \leqslant T_c, \tag{12}$$

while $f_q(T \geqslant T_c) = f_q(T_c)$. The nonanalytic behavior of f_q at T_c is a further characteristic feature of the mode-coupling singularity. Since we can easily take data for $T < T_c$ which are arguably not influenced by thermal vibrations, we can directly check for the presence of the square-root singularity, Eq. (12). This is done in the bottom panel of Fig. 8, where we also show data obtained from ND simulations. That the latter are strongly influenced by thermal vibrations is clear, since they systematically lie below the MC data and have a stronger temperature dependence close to T_c. However, even the MC data clearly indicate that $f_q(T)$ is better described by a nonsingular function of temperature, compatible with the simple linear behavior expected to hold at very low temperatures. The temperature dependence of the plateau height therefore explains why time temperature superposition does not hold in the late β regime, but the linear temperature

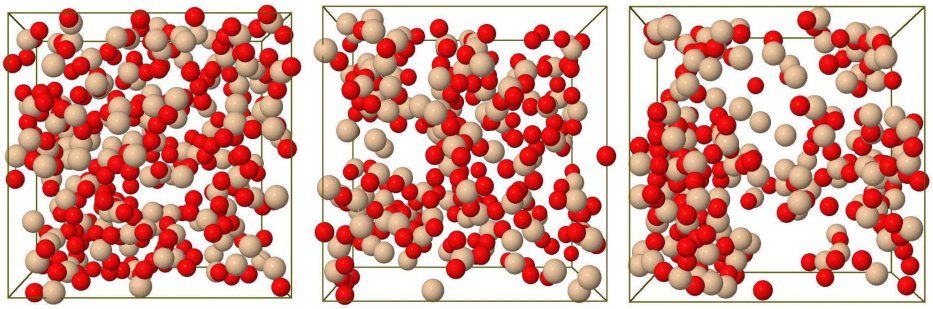

FIG. 9. (Color online) Snapshots of dynamic heterogeneity at $T=6100$, 3580, and 3000 K (from top to bottom). The snapshot presents particles which, in a particular run at a particular temperature have been slower than the average, and have therefore large, positive values of $\delta f_i(\mathbf{q},t\approx\tau_\alpha)$ defined in Eq. (15). Light shading is used for Si, dark shading for O. Slow particles tend to cluster in space on increasingly larger length scales when T decreases.

behavior indicates that there is no clear sign, from our data, of the existence of a "true" underlying singularity at T_c.

IV. DYNAMIC HETEROGENEITY

Having established the ability of MC simulations to efficiently reproduce the averaged slow dynamical behavior observed in ND simulations, we now turn to the study of the dynamic fluctuations around the average dynamical behavior, i.e., to dynamic heterogeneity.

Dynamic fluctuations can be studied through a four-point susceptibility, $\chi_4(t)$, which quantifies the strength of the spontaneous fluctuations around the average dynamics by their variance,

$$\chi_4(t) = N_\alpha[\langle f_s^2(\mathbf{q},t)\rangle - F_s^2(q,t)], \tag{13}$$

where

$$f_s(\mathbf{q},t) = \frac{1}{N_\alpha}\sum_{i=1}^{N_\alpha}\cos(\mathbf{q}\cdot[\mathbf{r}_i(t)-\mathbf{r}_i(0)]), \tag{14}$$

represents the real part of the instantaneous value of the self-intermediate scattering function, so that $F_s(q,t)=\langle f_s(\mathbf{q},t)\rangle$. As shown by Eq. (13), $\chi_4(t)$ will be large if run-to-run fluctuations of the self-intermediate scattering functions averaged in large but finite volume, are large. This is the case when the local dynamics becomes spatially correlated, as already discussed in several papers [35,43–48].

What $\chi_4(t)$ captures is information on the spatial structure of the spontaneous fluctuations of the dynamics around their average. We define $f_i(\mathbf{q},t)=\cos(\mathbf{q}\cdot[\mathbf{r}_i(t)-\mathbf{r}_i(0)])$, the contribution of particle i to the instantaneous value of $F_s(q,t)$, and

$$\delta f_i(\mathbf{q},t) = f_i(\mathbf{q},t) - F_s(q,t), \tag{15}$$

its fluctuating part. Then $\chi_4(t)$ can be rewritten in the suggestive form,

$$\chi_4(t) = \rho\int d\mathbf{r}\left\langle\sum_{i,j}\delta f_i(\mathbf{q},t)\,\delta f_j(\mathbf{q},t)\,\delta(\mathbf{r}-[\mathbf{r}_i(0)-\mathbf{r}_j(0)])\right\rangle, \tag{16}$$

where subtleties related to the exchange between the thermodynamic limit and the thermal average are discussed below. Therefore $\chi_4(t)$ is the volume integral of the spatial correlator between local fluctuations of the dynamical behavior of the particles. It gets larger when the spatial range of these correlations increases.

To get a view of what these fluctuations look like in real space, we present snapshots at different temperatures in Fig. 9. To build these snapshots we show, for a given run at a given temperature, those particles for which the fluctuating quantity $\delta f_i(\mathbf{q},t\approx\tau_\alpha)$, is positive and larger than a given threshold, which we choose close to 1/2 for graphical convenience (this leads to about 1/3 of the particles being shown, and clearer snapshots). The shown particles are therefore slower than the average for this particular run. The evolution of the snapshots between 6100 K and 3000 K clearly reveals the tendency for slow particles to cluster in space, revealing the growth of the length scale of kinetic heterogeneities. We should note, however, that the clusters shown here are not macroscopic objects even at the lowest temperature studied. Moreover, similar snapshots in Lennard-Jones systems reveal more clearly the tendency we seek to illustrate [35]. We interpret this as a further qualitative indication that dynamic heterogeneity is less pronounced in this strong material than in more fragile Lennard-Jones systems.

We turn to more quantitative measures of dynamic heterogeneity and show the time dependence of the dynamic susceptibility $\chi_4(t)$ obtained from our MC simulations for various temperatures in Fig. 10. Similar data are obtained for Si and O, and we only present the former. As predicted theoretically in Ref. [47] we find that $\chi_4(t)$ presents a complex time evolution, closely related to the time evolution of the self-intermediate scattering function. Overall, $\chi_4(t)$ is small at both small and large times when dynamic fluctuations are small. There is therefore a clear maximum observed for times comparable to τ_α, where fluctuations are most pronounced. The position of the maximum then shifts to larger times when temperature is decreased, tracking the α-relaxation time scale. The most important physical information revealed by these curves is the fact that the amplitude of the peak grows when the temperature decreases. This is direct evidence, recall Eq. (16), that spatial correlations grow when the glass transition is approached.

The two-step decay of the self-intermediate scattering function translates into a two-power law regime for $\chi_4(t)$

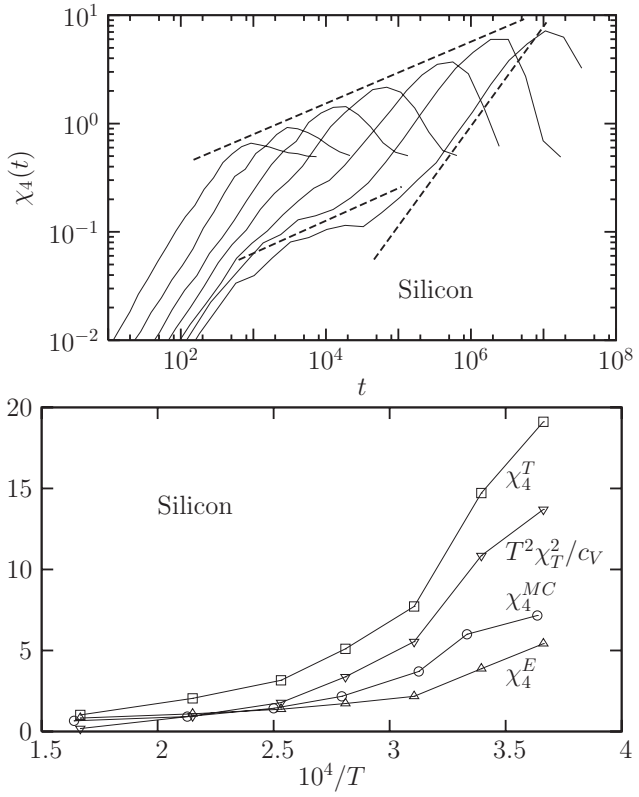

FIG. 10. Top: Four-point susceptibility, Eq. (13), for the same temperatures as in Fig. 2, decreasing from left to right. The low temperature data at $T=2750$ K are fitted with two power laws shown as dashed lines with exponents 0.3 and 0.92 at short and large times, respectively. The envelope of the maxima is fit with an exponent 0.285. Bottom: Temperature evolution of the maxima in various dynamic susceptibilities.

approaching its maximum. We have fitted these power laws, $\chi_4(t) \sim t^a$, followed by $\chi_4(t) \sim t^b$ with the exponents $a=0.3$ and $b=0.92$ in Fig. 10. We have intentionally used the notation a and b for these exponents which are predicted, within mode-coupling theory, to be equal to the standard exponents also describing the time dependence of intermediate scattering functions [4,47]. Our findings are in reasonable agreement with values for a and b discussed above, although the b value is about 50% too large. Moreover, a two-power law regime is only observed for $T<T_c$, where MCT does not apply anymore. We note that the b value is predicted to be $b=2$ from the perspective of modeling strong glass formers using kinetically constrained models with Arrhenius behavior [49]; this prediction is clearly incorrect for BKS silica [4,47].

We then focus on the amplitude of the dynamic susceptibility at its maximum and follow its temperature evolution in Fig. 10. As suggested by the snapshots shown in Fig. 9, we confirm that spatial correlations increase when T decreases, as χ_4 gets larger at low temperatures. The temperature evolution of the peak was discussed in Ref. [4]. Both MCT and kinetically constrained models strongly overestimate the temperature evolution of χ_4 at its peak value, as emphasized already in Ref. [4]. Finally, we note that the typical values observed for the peak of χ_4 at low temperatures are significantly smaller than those observed for more fragile Lennard-Jones systems, suggesting once more that dynamic heterogeneity is less pronounced in strong glass-forming materials.

This comparison is also useful to discuss the possibility of finite size effects on the present χ_4 data. If computed in a simulation box which is too small, the dynamic susceptibility takes values that are too small [50]. Our data indicate that no saturation of the maximum value of $\chi_4(t)$ is reached, and the values we find are smaller than the ones found in a Lennard-Jones system with a comparable system size and for which a detailed search for possible finite size effects was performed [3]. We believe therefore that our results are not affected by finite size effects.

We then compare these results to the ones obtained using Newtonian dynamics in the same system. In that case, care must be taken of the order at which the thermodynamic limit and the thermal average are taken in Eq. (16). Indeed when ND is used, the dynamics strictly conserves the energy during the simulation and thermal averages are then performed in the microcanonical ensemble, and χ_4^E is measured. To measure χ_4^T in the canonical ensemble for ND, an additional contribution must be added, which takes into account the amount of spontaneous fluctuations which are due to energy fluctuations [51],

$$\chi_4^T(t) - \chi_4^E(t) = \frac{T^2}{c_V}\left(\frac{\partial F_s(q,t)}{\partial T}\right)^2 \equiv \frac{T^2}{c_V}\chi_T(t), \qquad (17)$$

where c_V is the constant volume specific heat expressed in k_B units. The results for χ_4^T and χ_4^E obtained from ND, and the difference term in Eq. (17), are all presented in Fig. 10. We find that the MC results for χ_4 lie closer to the microcanonical results obtained from ND, while the canonical fluctuations are significantly larger, due to the large contribution of the right-hand side in Eq. (17). This is at first sight contrary to the intuition that MC simulations are thermostated and should be a fair representation of canonical averages in ND. But this is not what happens. As discussed in Refs. [3,4], a major role is played by conservation laws for energy and density when dynamic fluctuations are measured. In the case of energy conservation the mechanism can be physically understood as follows. For a rearrangement to take place in the liquid, the system must locally cross an energy barrier. If dynamics conserves the energy, particles involved in the rearrangement must borrow energy to the neighboring particles. This cooperativity might be unnecessary if energy can be locally supplied to the particles by an external heat bath, as in MC simulations. Conservation laws, therefore, might induce dynamic correlations between particles and dynamic fluctuations can be different when changing from Newtonian, energy conserving dynamics to a stochastic, thermostated dynamics. With hindsight, this is not such a surprising result. The specific heat, after all, also behaves differently in different statistical ensembles. The ensemble dependence and dependence upon the microscopic dynamics of dynamic susceptibilities in supercooled liquids are the main subjects of two recent papers [3,4]. Our results for silica quantitatively agree with the theoretical analysis they contain, and with the

corresponding numerical results obtained in Lennard-Jones systems.

There is an experimentally extremely relevant consequence of these findings [51,52]. As shown in Fig. 10, the difference between the microcanonical and canonical values of the dynamic fluctuations in ND represents in fact the major contribution to χ_4^T, meaning that the term χ_4^E can be safely neglected in Eq. (17). Since the right-hand side of (17) is more easily accessible in an experiment than χ_4^T itself, Eq. (17) opens the possibility of an experimental estimate of the four-point susceptibility. This finding, and its experimental application to supercooled glycerol and hard sphere colloids, constitute the central result of Ref. [51], while more data are presented in Ref. [52].

V. CONCLUSION

We have implemented a standard Monte Carlo algorithm to study the slow dynamics of the well-known BKS model for silica in the temperature range from 6100 K to 2750 K. Our results clearly establish that Monte Carlo simulations can be used to study the dynamics of silica because quantitative agreement is found with results from Newtonian dynamics for the same potential, apart at very short times where thermal vibrations are efficiently suppressed by the Monte Carlo algorithm. The agreement between the two dynamics is by no means trivial and constitutes an important result of the present study. This suggests that Monte Carlo simulations constitute a useful and efficient tool to study also the nonequilibrium aging dynamics of glass-forming liquids, a line of research initiated in Ref. [53].

Since dynamical correlations are not affected by short-time vibrations, we have been able to revisit the mode-coupling analysis initially performed in Ref. [13]. We find that mode-coupling theory accounts for the qualitative features of the data quite well, but the detailed, quantitative predictions made by the theory were shown to fail: correlation functions close to the plateau do not follow the behavior predicted for the MCT β correlator, time-temperature superposition only holds at very large times but fails at smaller times because the plateau in the correlation function is strongly temperature dependent, a dependence which does not follow the singular behavior predicted by MCT. Moreover, the temperature regime where the theory can supposedly be applied is found to be at most 1 decade when only the temperature evolution of relaxation time scales is considered. Furthermore, we have argued that the motivation to analyze silica data in terms of MCT, a "fragile to strong" crossover, can in fact be more simply accounted for in terms of a crossover between two distinct Arrhenius regimes occurring close to $T \approx 4000$ K. Overall these results suggest a negative answer to the question: is there any convincing evidence of an avoided mode-coupling singularity in silica?

We have finally analyzed dynamic heterogeneity in silica. We find that the dynamics is indeed spatially heterogeneous, and spatial correlation of the local dynamical behavior was shown to increase when temperature decreases. We also found that all indicators of dynamically heterogeneous dynamics such as decoupling and four-point dynamic susceptibilities, suggest that the effects are less pronounced in silica than in more fragile glass-forming materials, but do not seem qualitatively different.

The most natural interpretation is that strong and fragile materials in fact belong to the same class of materials, where the effects of dynamic heterogeneity could become less pronounced, but definitely nonzero, for materials with lower fragility. This suggests that it could be incorrect to assume that strong materials belong to a different universality class from fragile ones, as studies of kinetically constrained models with different fragilities would suggest [49,54], and they should rather appear at the end of the spectrum of fragile systems. It seems however similarly incorrect to consider that strong materials are "trivial" because an Arrhenius behavior can be explained from simple thermal activation over a fixed energy barrier corresponding to a local, noncooperative event. Our results show that this is not a correct representation of the physics of strong glass formers either. Convincingly incorporating fragility into current theories of the glass transition while simultaneously giving it a microscopic interpretation remains therefore an important challenge.

ACKNOWLEDGMENTS

This work emerged from collaboration with G. Biroli, J.-P. Bouchaud, W. Kob, K. Miyazaki, and D. Reichman [3,4]. D. Reichman offered the suggestion to revisit the MCT analysis of BKS silica, W. Kob helped with analyzing and interpreting the results, and A. Heuer made useful comments on the paper. This work has been supported in part by the Joint Theory Institute at Argonne National Laboratory and the University of Chicago.

[1] H. C. Andersen, Proc. Natl. Acad. Sci. U.S.A. **102**, 6686 (2005).
[2] M. Allen and D. Tildesley, *Computer Simulation of Liquids* (Oxford University Press, Oxford, 1987).
[3] L. Berthier, G. Biroli, J.-P. Bouchaud, W. Kob, K. Miyazaki, and D. R. Reichman, J. Chem. Phys. **126**, 184503 (2007).
[4] L. Berthier, G. Biroli, J.-P. Bouchaud, W. Kob, K. Miyazaki, and D. R. Reichman, J. Chem. Phys. **126**, 184504 (2007).
[5] S. P. Das and G. F. Mazenko, Phys. Rev. A **34**, 2265 (1986).
[6] G. Szamel and H. Löwen, Phys. Rev. A **44**, 8215 (1991).
[7] W. Götze, J. Phys.: Condens. Matter **11**, A1 (1999).
[8] W. Kob and H. C. Andersen, Phys. Rev. Lett. **73**, 1376 (1994); Phys. Rev. E **52**, 4134 (1995); Phys. Rev. E **51**, 4626 (1995).
[9] T. Gleim, W. Kob, and K. Binder, Phys. Rev. Lett. **81**, 4404 (1998).
[10] G. Szamel and E. Flenner, Europhys. Lett. **67**, 779 (2004).
[11] L. Berthier and W. Kob, J. Phys.: Condens. Matter **19**, 205130 (2007).

[12] B. W. H. van Beest, G. J. Kramer, and R. A. van Santen, Phys. Rev. Lett. **64**, 1955 (1990).
[13] J. Horbach and W. Kob, Phys. Rev. B **60**, 3169 (1999); Phys. Rev. E **64**, 041503 (2001).
[14] M. Vogel and S. C. Glotzer, Phys. Rev. Lett. **92**, 255901 (2004); Phys. Rev. E **70**, 061504 (2004).
[15] V. Teboul, A. Monteil, L. C. Fai, A. Kerrache, and S. Maabou, Eur. Phys. J. B **40**, 49 (2004).
[16] S. N. Taraskin and S. R. Elliott, Europhys. Lett. **39**, 37 (1997).
[17] M. Benoit, S. Ispas, P. Jund, and R. Jullien, Eur. Phys. J. B **13**, 631 (2000).
[18] K. Vollmayr, W. Kob, and K. Binder, Phys. Rev. B **54**, 15808 (1996).
[19] R. L. Mozzi and B. E. Warren, J. Appl. Crystallogr. **2**, 164 (1969).
[20] J. Horbach, Ph.D. thesis, University of Mainz, 1995 (unpublished).
[21] A. Carré, L. Berthier, J. Horbach, S. Ispas, and W. Kob, e-print arXiv:0707.0319.
[22] D. Wolf, Phys. Rev. Lett. **68**, 3315 (1992).
[23] D. Wolf, P. Keblimski, S. R. Phillpot, and J. Eggbrecht, J. Chem. Phys. **110**, 8254 (1999); C. J. Fennell and J. D. Gezeltzer, *ibid.* **124**, 234104 (2006).
[24] S. Whitelam and P. L. Geissler, e-print arXiv:cond-mat/0508100.
[25] Y. Zhang, G. Guo, K. Refson, and Y. Zhao, J. Phys.: Condens. Matter **16**, 9127 (2004).
[26] A. Saksaengwijit and A. Heuer, J. Phys.: Condens. Matter **19**, 205143 (2007).
[27] J. Horbach, W. Kob, K. Binder, and C. A. Angell, Phys. Rev. E **54**, R5897 (1996).
[28] M. Sellitto, G. Biroli, and C. Toninelli, Europhys. Lett. **69**, 496 (2005).
[29] G. Brébec, R. Seguin, C. Sella, J. Bevenot, and J. C. Martin, Acta Metall. **28**, 327 (1980); G. Urbain, Y. Bottinga, and P. Richet, Geochim. Cosmochim. Acta **46**, 1061 (1982); J. C. Mikkelsen, Appl. Phys. Lett. **45**, 1187 (1984).
[30] J.-L. Barrat, J. Badro, and P. Gillet, Mol. Simul. **20**, 17 (1997).
[31] I. Saika-Voivod, P. H. Poole, and F. Sciortino, Nature (London) **412**, 514 (2001).
[32] L. Berthier and J. P. Garrahan, Phys. Rev. E **68**, 041201 (2003).
[33] G. Tarjus, D. Kivelson, S. Mossa, and C. Alba-Simionesco, J. Chem. Phys. **120**, 6135 (2004).
[34] A. Saksaengwijit and A. Heuer, Phys. Rev. E **74**, 051502 (2006).
[35] L. Berthier, Phys. Rev. E **69**, 020201(R) (2004).
[36] L. Berthier, D. Chandler, and J. P. Garrahan, Europhys. Lett. **69**, 320 (2005).
[37] F. Fujara, B. Geil, H. Sillescu, and G. Fleischer, Z. Phys. B: Condens. Matter **88**, 195 (1992); M. T. Cicerone and M. D. Ediger, J. Chem. Phys. **103**, 5684 (1995); I. Chang and H. Sillescu, J. Phys. Chem. B **101**, 8794 (1997); S. F. Swallen, P. A. Bonvallet, R. J. McMahon, and M. D. Ediger, Phys. Rev. Lett. **90**, 015901 (2003).
[38] A. Andreanov, G. Biroli, and A. Lefèvre, J. Stat. Mech.: Theory Exp. (2006) P07008; M. E. Cates and S. Ramaswamy, Phys. Rev. Lett. **96**, 135701 (2006).
[39] L. J. Lewis and G. Wahnström, Phys. Rev. E **50**, 3865 (1994).
[40] A. Tanguy, J. P. Wittmer, F. Leonforte, and J.-L. Barrat, Phys. Rev. B **66**, 174205 (2002); F. Leonforte, A. Tanguy, J. P. Wittmer, and J.-L. Barrat, Phys. Rev. Lett. **97**, 055501 (2006).
[41] A. Saksaengwijit, J. Reinisch, and A. Heuer, Phys. Rev. Lett. **93**, 235701 (2004).
[42] T. Gleim and W. Kob, Eur. Phys. J. B **13**, 83 (2000).
[43] S. Franz and G. Parisi, J. Phys.: Condens. Matter **12**, 6335 (2000).
[44] S. Franz, C. Donati, G. Parisi, and S. C. Glotzer, Philos. Mag. B **79**, 1827 (1999).
[45] C. Bennemann, C. Donati, J. Baschnagel, and S. C. Glotzer, Nature (London) **399**, 246 (1999).
[46] N. Lačević, F. W. Starr, T. B. Schroder, and S. C. Glotzer, J. Chem. Phys. **119**, 7372 (2003).
[47] C. Toninelli, M. Wyart, L. Berthier, G. Biroli, and J.-P. Bouchaud, Phys. Rev. E **71**, 041505 (2005).
[48] P. Mayer, H. Bissig, L. Berthier, L. Cipelletti, J. P. Garrahan, P. Sollich, and V. Trappe, Phys. Rev. Lett. **93**, 115701 (2004).
[49] S. Whitelam, L. Berthier, and J. P. Garrahan, Phys. Rev. Lett. **92**, 185705 (2004); Phys. Rev. E **71**, 026128 (2005).
[50] L. Berthier, Phys. Rev. Lett. **91**, 055701 (2003).
[51] L. Berthier, G. Biroli, J.-P. Bouchaud, L. Cipelletti, D. El Masri, D. L'Hôte, F. Ladieu, and M. Pierno, Science **310**, 1797 (2005).
[52] C. Dalle-Ferrier, C. Thibierge, C. Alba-Simionesco, L. Berthier, G. Biroli, J.-P. Bouchaud, F. Ladieu, D. L'Hôte, and G. Tarjus, e-print arXiv:0706.1906.
[53] L. Berthier, Phys. Rev. Lett. **98**, 220601 (2007).
[54] J. P. Garrahan and D. Chandler, Phys. Rev. Lett. **89**, 035704 (2002); L. Berthier and J. P. Garrahan, J. Phys. Chem. B **109**, 3578 (2005).